Perfringolysin O as a useful tool to study human sperm physiology

Cristián A. Pocognoni, M.S.,[a] Gerardo A. De Blas, Ph.D.,[a] Alejandro P. Heuck, Ph.D.,[b] Silvia A. Belmonte, Ph.D.,[a] and Luis S. Mayorga, Ph.D.[a]

[a] IHEM (CONICET-UNCuyo), School of Medicine, National University of Cuyo, Mendoza, Argentina; and [b] Department of Biochemistry and Molecular Biology, University of Massachusetts, Amherst, Massachusetts

Objective: To evaluate perfringolysin O, a cholesterol-dependent pore-forming cytolysin, as a tool to study several aspects of human sperm physiology.
Design: Prospective study.
Setting: Basic research laboratory.
Patient(s): Human semen samples with normal parameters obtained from healthy donors.
Intervention(s): Interaction of recombinant perfringolysin O with human spermatozoa.
Main Outcome Measure(s): Assessment of perfringolysin O binding to spermatozoa, tests for acrosome and plasma membrane integrity, and acrosomal exocytosis assays.
Result(s): Perfringolysin O associated with human spermatozoa at 4°C. The binding was sensitive to changes in cholesterol concentrations and distribution occurring in the plasma membrane of these cells during capacitation. When perfringolysin O–treated sperm were incubated at 37°C, the plasma membrane became permeable, whereas the acrosome membrane remained intact. Permeabilized spermatozoa were able to respond to exocytic stimuli. The process was inhibited by proteins that interfere with membrane fusion, indicating that large molecules, including antibodies, were able to permeate into the spermatozoa.
Conclusion(s): PFO is a useful probe to assess changes in the amount and distribution of the active sterol fraction present in the sperm plasma membrane. The toxin can be used for the efficient and selective permeabilization of this membrane, rendering a flexible experimental model suitable for studying molecular processes occurring in the sperm cytoplasm. (Fertil Steril® 2013;99:99–106. ©2013 by American Society for Reproductive Medicine.)
Key Words: Perfringolysin O, cholesterol, acrosome reaction, human sperm, permeabilization

Discuss: You can discuss this article with its authors and with other ASRM members at http://fertstertforum.com/pocognonica-perfringolysin-o-sperm-physiology/

Use your smartphone to scan this QR code and connect to the discussion forum for this article now.*

* Download a free QR code scanner by searching for "QR scanner" in your smartphone's app store or app marketplace.

Spermatozoon, the male gamete, is a highly differentiated cell capable of finding the female gamete, sorting through all the physical barriers that protect this immobile cell, and fusing with the oocyte to generate a diploid zygote (1). To perform these complex tasks, the spermatozoon undergoes dramatic morphological and functional changes during spermiogenesis, resulting in a very specialized cell capable of carrying out a limited set of functions with high efficiency. Sperm are excellent model cells to dissect fundamental processes such as flagellum-mediated cell motility (2), chemotaxis (3–5), and regulated exocytosis (6, 7). Therefore, unveiling the molecular mechanisms underlying these cellular functions in sperm is of great interest not only to address specific problems in reproductive biology but also to understand key processes in cell biology.

In mammals, ejaculated sperm are unable to respond properly to stimuli coming from the oocyte. They have to undergo a complex capacitation process in the female reproductive tract to acquire special functions that are important for fertilization, such as hyperactivated motility and the ability to respond to acrosome reaction inducers (8). Several important changes occur at the sperm's plasma membrane during capacitation, such as hyperpolarization, opening of voltage-gated calcium channels, loss of transbilayer phospholipid asymmetry (9), and efflux of cholesterol (for a review, see Flesch and Gadella, [10]). Cholesterol contents decrease up to 40% in various mammalian sperm capacitated in vitro (10). Our

Received June 25, 2012; revised August 9, 2012; accepted August 22, 2012; published online September 19, 2012.
C.A.P. has nothing to disclose. G.A.D.B. has nothing to disclose. A.P.H. has nothing to disclose. S.A.B. has nothing to disclose. L.S.M. has nothing to disclose.
This work was supported by grants from the National University of Cuyo, Argentina (06/J388 and 06/J353 SeCTyP), CONICET, Argentina (PIP 112-200801-02277), and ANPCyT, Argentina (PICT-2008-1114 and PICT-2010-1789).
Reprint requests: Luis S. Mayorga, Ph.D., Casilla Correo 56, 5500 Mendoza, Argentina (E-mail: lmayorga@fcm.uncu.edu.ar).

Fertility and Sterility® Vol. 99, No. 1, January 2013 0015-0282/$36.00

http://dx.doi.org/10.1016/j.fertnstert.2012.08.052

laboratory demonstrated that cholesterol efflux facilitates the exocytosis of the acrosome by favoring Rab3A membrane association (11). The regulation of cholesterol levels is important for the function of these cells. Hypercholesterolemia decreases male factor fertility in animal models, altering several sperm parameters (12, 13). Dyslipidemia also has an impact on human male factor fertility (14–16).

Acrosomal exocytosis is fundamental for gamete interactions and fusion (1). Sperm have a single, flat, and large secretory granule surrounding the anterior part of the nucleus. Similar to exocytic events occurring in other secretory cells, the plasma membrane and the granule membrane fuse during the acrosome reaction to release the granule contents. However, acrosomal exocytosis is special in several aspects. Upon stimulation, multiple fusion pores between the outer acrosomal membrane and the plasma membrane form, connecting the interior of the acrosome with the extracellular medium. By a still not well characterized process, these fusion pores expand, causing the fenestration of both membranes and the release of hybrid vesicles composed of patches of plasma membrane and outer acrosomal membrane (17).

A drawback for experiments with spermatozoa is the limited, almost null, transcriptional and translational activity of these cells. As a result, protein overexpression and knockdown are difficult and require the generation of transgenic animals, which is experimentally demanding for most species and prohibitive for human sperm. Controlled plasma membrane permeabilization has been used to gain access to the membrane fusion machinery required for exocytosis in several secretory cells (18, 19). We and others have resorted to this strategy to study the molecular aspects of sperm physiology (20–22).

The aim of the present work was to characterize perfringolysin O (PFO) as a useful tool to study several aspects of sperm physiology. PFO is a pore-forming toxin secreted by *Clostridium perfringens* (23). It belongs to the family of cholesterol-dependent cytolysins (24). After binding to sterol-containing membranes via the C-terminal domain (25), PFO oligomerizes forming a large prepore complex composed of up to 50 monomers (26) and inserts a transmembrane β-barrel of approximately 25 nm in diameter (27). Our goal was to explore the possibility of using the cholesterol-binding and pore-forming properties of this protein to investigate changes in cholesterol availability during capacitation and to study the molecular mechanism of acrosomal exocytosis.

MATERIALS AND METHODS

Additional Materials and Methods information can be found in Supplemental Materials (available online).

Recombinant PFO

The plasmid pAH11 encoding His_6-tagged native PFO (28) was transformed into *Escherichia coli* strain BL21 (DE3) pLysS. Protein synthesis was induced 2.5 hours at 37°C with 1 mM isopropyl beta-D-1-thiogalactopyranoside (IPTG). Bacteria were harvested and lysed by sonication, and PFO was purified under native conditions by affinity chromatography on Ni-NTA-agarose. PFO preparations (about 1 μM) were divided in 15 μL aliquots and stored at −80°C in elution buffer (250 mM imidazole, 100 mM NaCl, 50 mM Tris-HCl, pH 8). Under these storage conditions, PFO was stable and fully active for at least 6 months.

Sperm

Human semen samples were provided by masturbation from 15 healthy volunteer donors. The informed consent signed by the donors and the protocol for semen sample handling were approved by the Ethics Committee of the School of Medicine, National University of Cuyo. At least 120 sperm samples were used to perform this work. After sample liquefaction (20–30 minutes at 37°C), highly motile sperm were recovered by swim-up separation for 1.5 hours in human tubal fluid media (HTF, as formulated by Irvine Scientific) at 37°C in an atmosphere of 5% CO_2/95% air. The sperm suspension was diluted with HTF to 7×10^6 sperm/mL and incubated under the same conditions for 2–3 hours. When capacitated sperm were required, HTF was supplemented with 5 mg/mL bovine serum albumin (BSA) during the swim-up and the postdilution incubation.

PFO Binding to Sperm Plasma Membrane

Capacitated and noncapacitated spermatozoa were washed twice, resuspended in ice-cold phosphate-buffered saline (PBS) containing 25 nM PFO, and incubated for 15 minutes at 4°C. After washing twice with PBS to remove the free toxin, the cells were either fixed for immunofluorescence assays or solubilized for Western blot analysis (details in Supplemental Materials).

Plasma Membrane Permeabilization with PFO

Capacitated spermatozoa were washed twice, resuspended in ice-cold PBS containing 25 nM PFO, and incubated for 15 minutes at 4°C. After washing twice with PBS to remove the unbound toxin, the cells were resuspended (7×10^6/mL) in ice-cold HB-EGTA buffer (250 mM sucrose, 0.5 mM EGTA, 20 mM Hepes-K, pH 7) containing (or not) 2 mM dithiothreitol (DTT). After incubation at 37°C for different times (15 minutes when not indicated otherwise), permeabilization was assessed using 0.1% eosin Y or 500 nM propidium iodide (both in HB-EGTA).

RESULTS

PFO Bound Differentially to Capacitated and Noncapacitated Sperm Cells

Sperm capacitation in mammals requires an efflux of cholesterol from the plasma membrane. We tested whether PFO was able to detect the difference in cholesterol content between noncapacitated and capacitated sperm. For this purpose, the pore-forming property of the toxin was inhibited by incubating spermatozoa with PFO at low temperature (4°C) in the absence of reducing agents. Under these conditions, the toxin associated with both capacitated and noncapacitated sperm as assessed by Western blot analysis. The binding was more efficient for noncapacitated sperm as would be expected owing to the higher cholesterol contents of these cells (Fig. 1A,

FIGURE 1

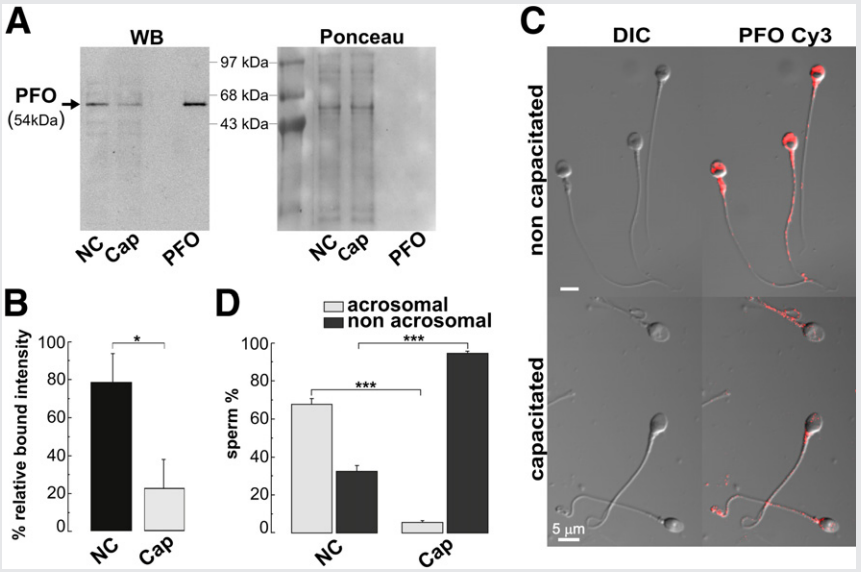

PFO detected changes in the cholesterol accessibility at the plasma membrane of human sperm. (A) Human sperm (7×10^6 cells) incubated under capacitating (Cap) or noncapacitating (NC) conditions were incubated with 25 nM PFO at 4°C for 15 minutes. The cells were washed, and sperm extracts were prepared and resolved in 10% tricine gels, transferred to nitrocellulose membranes, and probed with an anti-His_6 antibody (left). Recombinant PFO (650 ng) was included as a control. The membrane stained with Ponceau *red* is shown on the right panel. Molecular weight markers are indicated between both panels, and PFO expected molecular weight is on the left. (B) Quantification of two Western blots similar to the one shown in panel A. Data represent the mean ± range of two independent experiments. *Significant difference for $P<.05$ (Student's *t*-test). (C) Spermatozoa treated as in panel A (noncapacitated, *top panel*; capacitated, *bottom panel*) were spotted on coverslips, fixed, and immunolabeled with the anti-His_6 antibody. Bars = 5 μm. (D) The immunostaining patterns for spermatozoa treated as in panel B were classified as "acrosomal" (clear stain at the acrosomal region) or "nonacrosomal" (lack of label at the acrosomal region) in at least 100 cells and expressed as a percentage of the total. Data represent the mean ± SEM of three independent experiments. ***Significant difference for $P<.01$ (Student's *t*-test).

Pocognoni. Perfringolysin O interaction with human spermatozoa. Fertil Steril 2013.

left panel). Notice that the protein loads were similar in capacitated and noncapacitated sperm (Fig. 1A, right panel). The intensity of the bands was quantified by densitometry, and the results are shown in Figure 1B. By indirect immunofluorescence, the binding of the toxin also showed significant differences between capacitated and noncapacitated sperm. A label was evident in the acrosomal region of most noncapacitated sperm (Fig. 1C, upper panel, quantified in Fig. 1D) that almost disappeared after capacitation (Fig. 1C, lower panel, quantified in Fig. 1D).

PFO Forms Pores in Sperm Plasma Membrane

We designed a protocol to generate pores in the plasma membrane to gain access to the cytoplasmic compartment of human sperm. The rationale for the protocol is the following. Recombinant PFO associates with cholesterol-containing membranes with high efficiency even at 4°C (Fig. 1). Therefore, the first step in the protocol was to incubate the toxin with human spermatozoa at 4°C. Notice that under these conditions, the toxin did not perforate the plasma membrane, which served as a barrier preventing the interaction with inner compartments. Unbound toxin was eliminated by washing. The cells were resuspended in a sucrose buffer, which stabilizes intracellular organelles (29), containing a low calcium concentration to mimic the intracellular contents of this ion (free calcium concentration in the reaction mixture was on the order of 10^{-7} M) and supplemented with DTT to preserve the reducing condition of the cytoplasm. Cells were then incubated at 37°C for different periods of time to promote toxin-mediated pore formation in the plasma membrane. This protocol was tested adjusting PFO concentrations and the time of incubation at 37°C and assessing permeabilization by incorporation of the supravital dye eosin Y. As shown in Figure 2A, the toxin efficiently permeabilized spermatozoa after 10 minutes of incubation (ED50 9 ± 3 nM at 10 minutes, 8 ± 3 at 15 minutes). PFO was significantly less potent when the incubation time was reduced to 5 minutes (ED50 37 ± 7 nM), indicating that this time of incubation was not sufficient to complete the permeabilization process. We tested whether reducing conditions were necessary for cell permeabilization. As shown in Figure 2B, the presence of DTT significantly increased the percentage of permeabilized sperm at the three incubation times tested, indicating that Cys459 may become oxidized during purification and storage of the toxin (27). Interestingly, despite the fact that cholesterol accessibility was reduced on capacitated sperm, PFO was still able to bind and permeabilize the plasma membrane.

To test whether the permeabilization protocol affected the acrosomal membrane, sperm cells were incubated under three conditions: [1] no additions (which should affect neither the plasma nor the acrosomal membrane), [2] treated with PFO

FIGURE 2

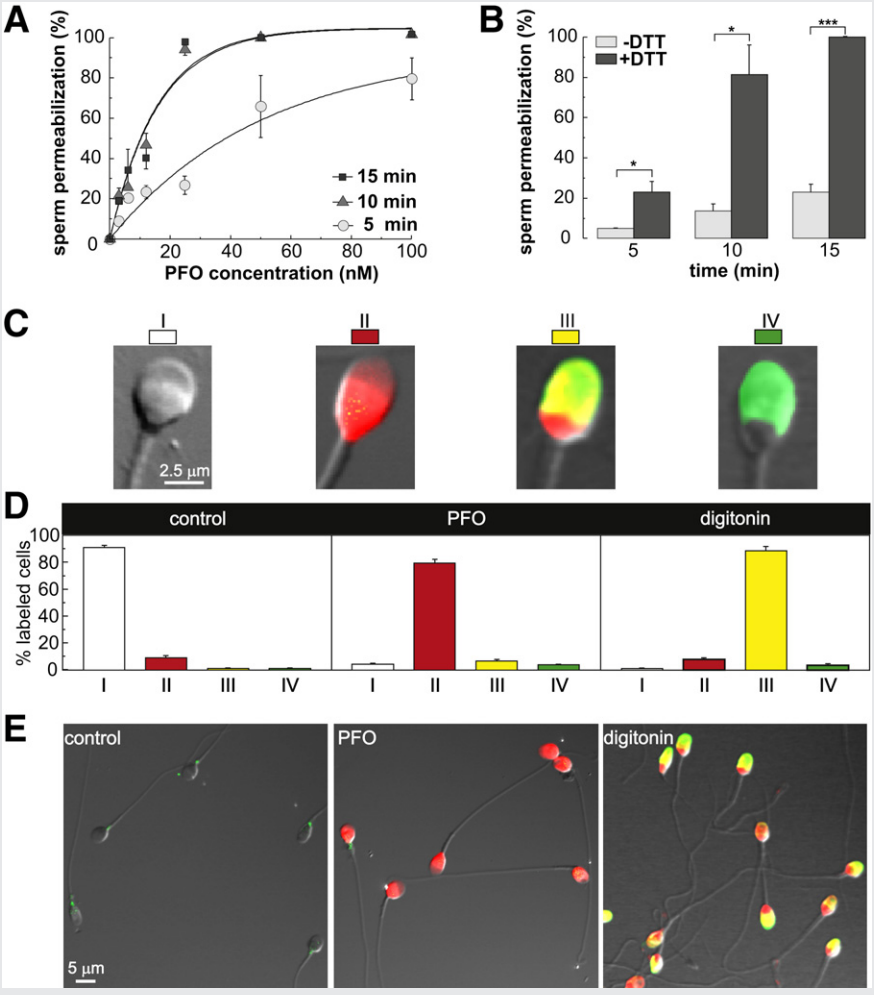

PFO efficiently and specifically permeabilizes the human sperm plasma membrane. (A) Spermatozoa capacitated for 3 hours were incubated with increasing PFO concentrations (0–100 nM) for 15 minutes at 4°C in PBS. The cells were washed and resuspended in HB-EGTA containing 2 mM DTT and incubated for 5, 10, or 15 minutes at 37°C. Permeabilization was assessed by using the vital dye eosin Y (0.1% in HB-EGTA). At least 100 cells were scored, and the number of permeabilized cells was expressed as a percentage of the total. (B) Capacitated sperm were treated with 25 nM PFO as explained in panel A and resuspended in HB-EGTA containing (+DTT) or not (−DTT) 2 mM DTT and incubated for 5, 10, and 15 minutes at 37°C. Permeabilization was assessed as in panel A. Data in panels A and B represent the mean ± SEM of three independent experiments. * and ***Significant difference for $P<.05$ and $P<.001$, respectively (Student's *t*-test). To assess the integrity of sperm membranes, capacitated human sperm were incubated in PBS without addition (control) or supplemented with 25 nM PFO (PFO) or 50 μM digitonin (digitonin). Sperm were washed and resuspended in HB-EGTA containing 2 mM DTT, 5 μg/mL PSL-FITC (to test acrosomal membrane permeability), and 1 μg/mL propidium iodide (to test plasma membrane permeability). After 15 minutes at 37°C, cells were washed once, spotted on coverslips, and fixed. Sperm were analyzed in a confocal microscope, and the images were recorded in the DIC, FITC (*green*), and propidium iodide (*red*) channels. (C) Four staining patterns were considered in the experiment. I: Unstained spermatozoon (intact acrosomal and plasma membranes); II: *red* nucleus (permeabilized plasma membrane and intact acrosomal membrane); III: *red* nucleus and *green* acrosome (permeabilized acrosomal and plasma membranes); IV: *green* acrosome (intact plasma membrane and permeabilized acrosome); bar = 2.5 μm. (D). Percentage of sperm showing the patterns defined in panel A under the experimental conditions described above: untreated (control), treated with PFO (PFO), or treated with digitonin (digitonin). The bars represent the mean ± SEM of three independent experiments. (E) Representative microscopic fields for each treatment (DIC, *green*, and *red* channels combined; bar = 5 μm).

Pocognoni. Perfringolysin O interaction with human spermatozoa. Fertil Steril 2013.

(which should only permeabilize the plasma membrane), and [3] treated with digitonin (which should permeabilize the plasma and the acrosomal membranes). The integrity of the plasma membrane was assessed using the membrane-impermeable nuclear stain propidium iodide, and damage to the acrosomal membrane was visualized with *Pisum sativum* agglutinin conjugated with fluorescein isothiocyanate (PSL-FITC), which should only gain access to the acrosomal lumen when the membrane of this organelle is affected (staining patterns are shown in Fig. 2C). The treatment with PFO strongly increased the percentage of sperm with permeabilized plasma membrane and intact acrosomal membrane. In contrast, digitonin permeabilized both membranes (Fig. 2D and E). These results clearly show that PFO selectivity

permeabilized the sperm plasma membrane and did not affect the acrosomal membrane.

PFO Permeabilization Recorded in Real Time

Next we set out to follow the dynamics of PFO-induced permeabilization in individual spermatozoa in real time. For this purpose, cells were immobilized on coverslips coated with polylysine and incubated at 37°C in HB-EGTA medium containing 500 nM propidium iodide. The process was followed under the microscope for 15 minutes, and images were collected every 10 seconds. The plasma membrane was not affected by incubating sperm in HB-EGTA in the absence (Fig. 3A, control) or presence of 2 mM DTT (Fig. 3A, DTT). In contrast, when 25 nM PFO was added after 0.5 minutes of incubation, spermatozoa started to incorporate propidium iodide (Fig. 3A, PFO + DTT). By using this protocol (Fig. 3B, 3C, and 3D), the permeabilization efficiency was lower than that reported in Figure 2, probably because spermatozoa were not preincubated with the toxin at 4°C. The analysis of propidium iodide incorporation in individual cells showed some interesting features. The kinetics was similar for all

FIGURE 3

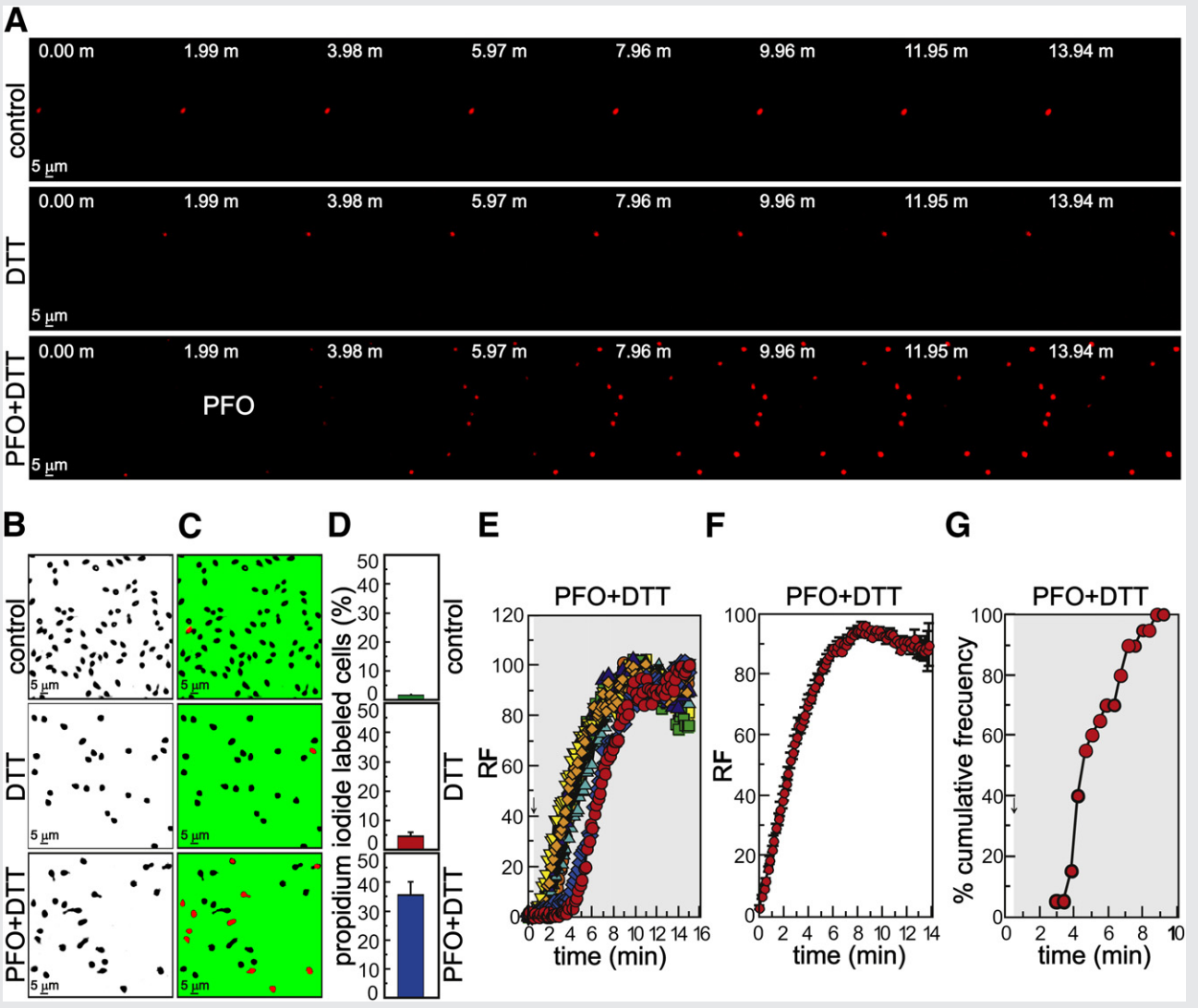

Effect of PFO on plasma membrane permeability recorded in real time. Capacitated human sperm were immobilized on coverslips with polylysine and incubated at 37°C in HB-EGTA containing 500 nM propidium iodide (control) and supplemented, when indicated, with 2 mM DTT (DTT). In some experiments, PFO (25 nM) was added after 30 seconds of incubation (PFO + DTT). Sequential images were captured every 10 seconds. (A) Representative fields showing changes of propidium iodide incorporation under the three different conditions. (B) Phase contrast of the same fields shown in panel A after 15 minutes of incubation. (C) Pseudocolor of merged images (phase contrast and propidium iodide) of the same fields shown in panel B. (D) Quantification of the percentage of permeabilized cells under the three conditions (media ± SEM, n = 3). (E) Relative fluorescence intensity (RF) in single sperm after the addition of PFO (PFO + DTT). (F) Average relative fluorescence intensity for all spermatozoa. The series were synchronized to the time of the initial fluorescence increase. (G) Permeabilization time for individual sperm represented by the cumulative frequency of the time required for each sperm to acquire 50% of the maximal fluorescence intensity.

Pocognoni. Perfringolysin O interaction with human spermatozoa. Fertil Steril 2013.

spermatozoa; when the process started, about 68% of propidium iodide was incorporated in 2 minutes (Fig. 4F). However, not all spermatozoa where permeabilized simultaneously; some cells underwent permeabilization after a short delay (3 minutes), whereas for others, the latency period was longer (9 minutes, Fig. 3G).

PFO-Permeabilized Sperm Can Be Used to Study Acrosomal Exocytosis

We then tested whether PFO-permeabilized sperm were able to undergo acrosomal exocytosis and whether the process could be modulated by membrane-impermeable reagents. As shown in Figure 4, calcium and recombinant, preactivated Rab3A triggered exocytosis in PFO-permeabilized sperm but not in intact cells. Moreover, calcium-triggered exocytosis was inhibited by antibodies that inactivate endogenous Rab3A, complexin, and Epac (Fig. 4), three proteins that are necessary for the process (21, 30). The Rab3A-GTP binding cassette RIM-RBD, which sequesters the active form of Rab3 (31), also inhibited secretion. Notice that even large proteins, such as IgGs (MW about 150,000), were able to permeate into the cell through the PFO pores. These results indicated that the permeabilization procedure did not inactivate the secretory process and preserved the membrane fusion machinery that is required for exocytosis.

DISCUSSION

Membrane cholesterol plays an important role in sperm physiology (9, 12–16). Sterols form complexes with polar bilayer lipids, mostly phospholipids, with diverse affinities. The possibility of forming these complexes is limited; the sterol fraction that exceeds the complexing capacity of the polar bilayer lipids is called "active" (32). The efflux of cholesterol occurring during capacitation probably affects mostly the active fraction of the lipid, which has an increased escape tendency. PFO binding to cellular membranes depends on active sterols (28, 33–35); hence, this protein is a useful probe to sense changes in the amount and distribution of the active fraction of membrane sterols. Based on Western blot and indirect immunofluorescence experiments, we report here that full-length PFO binds to human spermatozoa and that binding is strongly affected by capacitation. We observed by immunofluorescence that PFO specifically associates to the acrosomal region of the plasma membrane in noncapacitated sperm and that capacitation strongly decreased the labeling in this area. Other groups have shown that that the cholesterol-binding domain of PFO fused to green fluorescent protein binds mouse and human spermatozoa in the acrosomal region (36). By using filipin, a fluorescent cholesterol-binding antibiotic, it has been shown that capacitation decreases labeling in this region (9). We conclude that our observations are consistent with physiological changes occurring during capacitation and with the results of other groups using different probes; hence we propose that recombinant full-length PFO is a useful probe to assess changes in the amount and distribution of the active sterol fraction in the sperm plasma membrane.

In this report we show that PFO is suitable for human sperm permeabilization. When the plasma membrane-bound toxin was activated, the membrane-impermeable dyes eosin Y and propidium iodide were able to permeate into the sperm.

FIGURE 4

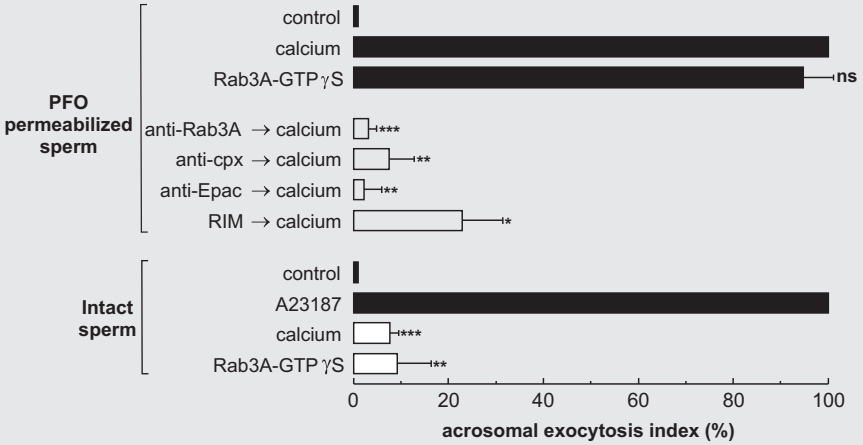

Acrosomal exocytosis in PFO-permeabilized sperm. Capacitated spermatozoa were permeabilized with 25 nM PFO, resuspended in HB-EGTA containing 2 mM DTT (PFO-permeabilized sperm), and incubated for 10 minutes at 37°C with the following membrane impermeable inhibitors: 66 nM anti-Rab3A antibody (anti-Rab3A), 34 nM anti-complexin I/II antibody (anti-cpx), 7 nM anti-Epac antibody (anti-Epac), and 74 nM Rab3A-GTP binding cassette (RIM). Afterward, the cells were incubated for 10 minutes without stimulus (control) or with the membrane-impermeable activators calcium (10 μM free calcium) or Rab3A-GTPγS (300 nM). The same activators at the same concentration were tested in nonpermeabilized capacitated spermatozoa (intact sperm) in HTF medium. Calcium ionofore A23187 (10 μM) was used as positive control for intact spermatozoa. At the end of the incubation, acrosomal exocytosis was evaluated using PSL-FITC, and data were normalized as described in the Supplemental Materials. The data represent mean ± SEM of at least three independent experiments. The means were compared with the respective control by using one-way analysis of variance and the Dunnett test (*, **, and ***Significantly different from 100% for $P<.05$, $P<.01$, and $P<.001$, respectively; ns = not significantly different).

Pocognoni. Perfringolysin O interaction with human spermatozoa. Fertil Steril 2013.

In contrast, PSL-FITC was not incorporated into the acrosome, showing that the membrane of this organelle was intact. The dose-response curves and the real time permeabilization experiments indicate that approximately 10 minutes at 37°C is necessary to complete the permeabilization process. Not all spermatozoa were permeabilized at the same time. Whether this heterogeneity reflects differences in the cholesterol content of the individual spermatozoa remains to be investigated.

The protocol described is suitable for a selective plasma membrane permeabilization and good preservation of the acrosome's integrity. Moreover, functional assays indicate that the molecular mechanisms for acrosomal exocytosis were maintained. The presence of PFO pores in the plasma membrane enabled us to manipulate the exocytic process by including relatively large proteins in the extracellular medium. Inhibition of endogenous Rab3A by an inactivating antibody (31) or by sequestering the GTP-bound form of this protein using a domain of RIM1α (31) inhibited calcium-triggered exocytosis. A specific antibody against Epac—a cAMP-regulated protein that plays a central role in an early step of acrosomal exocytosis (37)—also blocked secretion. Complexin is required to stabilize SNARE complexes, which are at the core of the molecular mechanism responsible for the opening of fusion pores (38). An antibody that recognizes complexin I and II was also able to abrogate acrosomal exocytosis. The effect of all these proteins, which affect different steps of the exocytic process, indicates that PFO permeabilized spermatozoa remain functionally active and can incorporate relatively large proteins that permeate through the pores opened in the plasma membrane.

PFO has been used for permeabilizing other cell types (39–42), although far less frequently than streptolysin O (SLO), another cholesterol-dependent cytolysin. We have also developed a protocol to permeabilize human and mouse sperm with SLO (30, 43). However, not all SLO preparations are suitable. Acrosomal exocytosis was not always functional upon permeabilization with some commercially available SLO preparations. Moreover, the permeabilization potency of the preparations was batch dependent and changed with time (unpublished observations). In our hands, PFO tagged with His_6 produced as a recombinant protein and purified by standard procedures was suitable for sterol binding and sperm permeabilization. We have worked with four different batches and obtained similar results.

In conclusion, we have shown that PFO is a useful tool to detect active cholesterol in the sperm plasma membrane and for the efficient and selective permeabilization of this membrane. We expect that this toxin will foster the understanding of several physiological processes in these unique cells.

Acknowledgments: The authors thank Graciela Gutierrez, Alejandra Medero, and Marcelo Furlán for excellent technical assistance and Claudia Tomes for critically reading the manuscript.

REFERENCES

1. Yanagimachi R. Mammalian Fertilization. In: Knobil E, Neill JD, editors. The physiology of reproduction. New York: Raven Press; 1994:189–281.
2. Lesich KA, Pelle DW, Lindemann CB. Insights into the mechanism of ADP action on flagellar motility derived from studies on bull sperm. Biophys J 2008; 95:472–82.
3. Guerrero A, Nishigaki T, Carneiro J, Yoshiro T, Wood CD, Darszon A. Tuning sperm chemotaxis by calcium burst timing. Dev Biol 2010;344:52–65.
4. Alvarez L, Dai L, Friedrich BM, Kashikar ND, Gregor I, Pascal R, Kaupp UB. The rate of change in Ca^{2+} concentration controls sperm chemotaxis. J Cell Biol 2012;196:653–63.
5. Blengini CS, Teves ME, Unates DR, Guidobaldi HA, Gatica LV, Giojalas LC. Human sperm pattern of movement during chemotactic re-orientation towards a progesterone source. Asian J Androl 2011;13:769–73.
6. Mayorga LS, Tomes CN, Belmonte SA. Acrosomal exocytosis, a special type of regulated secretion. IUBMB Life 2007;59:286–92.
7. Tomes C. Acrosomal exocytosis. In: Regazzi R, editor. Molecular mechanisms of exocytosis. Georgetown: Landes Bioscience; 2007:117–47.
8. Visconti PE, Krapf D, de la Vega-Beltran JL, Acevedo JJ, Darszon A. Ion channels, phosphorylation and mammalian sperm capacitation. Asian J Androl 2011;13:395–405.
9. Flesch FM, Brouwers JF, Nievelstein PF, Verkleij AJ, van Golde LM, Colenbrander B, et al. Bicarbonate stimulated phospholipid scrambling induces cholesterol redistribution and enables cholesterol depletion in the sperm plasma membrane. J Cell Sci 2001;114:3543–55.
10. Flesch FM, Gadella BM. Dynamics of the mammalian sperm plasma membrane in the process of fertilization. Biochim Biophys Acta 2000;1469: 197–235.
11. Belmonte SA, Lopez CI, Roggero CM, De Blas GA, Tomes CN, Mayorga LS. Cholesterol content regulates acrosomal exocytosis by enhancing Rab3A plasma membrane association. Dev Biol 2005;285:393–408.
12. Shalaby MA, el-Zorba HY, Kamel GM. Effect of alpha-tocopherol and simvastatin on male fertility in hypercholesterolemic rats. Pharmacol Res 2004;50:137–42.
13. Saez Lancellotti TE, Boarelli PV, Monclus MA, Cabrillana ME, Clementi MA, Espinola LS, et al. Hypercholesterolemia impaired sperm functionality in rabbits. PLoS ONE 2010;5:e13457.
14. Ramirez-Torres MA, Carrera A, Zambrana M. High incidence of hyperestrogenemia and dyslipidemia in a group of infertile men. Ginecol Obstet Mex 2000;68:224–9.
15. Kasturi SS, Tannir J, Brannigan RE. The metabolic syndrome and male infertility. J Androl 2008;29:251–9.
16. Buffone MG, Verstraeten SV, Calamera JC, Doncel GF. High cholesterol content and decreased membrane fluidity in human spermatozoa are associated with protein tyrosine phosphorylation and functional deficiencies. J Androl 2009;30:552–8.
17. Zanetti N, Mayorga LS. Acrosomal swelling and membrane docking are required for hybrid vesicle formation during the human sperm acrosome reaction. Biol Reprod 2009;81:396–405.
18. Zheng Q, Bobich JA, Vidugiriene J, McFadden SC, Thomas F, Roder J, et al. Neuronal calcium sensor-1 facilitates neuronal exocytosis through phosphatidylinositol 4-kinase. J Neurochem 2005;92:442–51.
19. Hafez I, Stolpe A, Lindau M. Compound exocytosis and cumulative fusion in eosinophils. J Biol Chem 2003;278:44921–8.
20. Hutt DM, Baltz JM, Ngsee JK. Synaptotagmin VI and VIII and syntaxin 2 are essential for the mouse sperm acrosome reaction. J Biol Chem 2005;280: 20197–203.
21. Michaut M, Tomes CN, De Blas G, Yunes R, Mayorga LS. Calcium-triggered acrosomal exocytosis in human spermatozoa requires the coordinated activation of Rab3A and N-ethylmaleimide-sensitive factor. Proc Natl Acad Sci U S A 2000;97:9996–10001.
22. Johnson LR, Moss SB, Gerton GL. Maintenance of motility in mouse sperm permeabilized with streptolysin O. Biol Reprod 1999;60:683–90.
23. Tweten RK. Cholesterol-dependent cytolysins, a family of versatile pore-forming toxins. Infect Immun 2005;73:6199–209.
24. Heuck AP, Moe PC, Johnson BB. The cholesterol-dependent cytolysin family of gram-positive bacterial toxins. Subcell Biochem 2010;51:551–77.
25. Ramachandran R, Heuck AP, Tweten RK, Johnson AE. Structural insights into the membrane-anchoring mechanism of a cholesterol-dependent cytolysin. Nat Struct Biol 2002;9:823–7.

26. Shepard LA, Shatursky O, Johnson AE, Tweten RK. The mechanism of pore assembly for a cholesterol-dependent cytolysin: formation of a large prepore complex precedes the insertion of the transmembrane beta-hairpins. Biochemistry 2000;39:10284–93.
27. Shatursky O, Heuck AP, Shepard LA, Rossjohn J, Parker MW, Johnson AE, et al. The mechanism of membrane insertion for a cholesterol-dependent cytolysin: a novel paradigm for pore-forming toxins. Cell 1999;99:293–9.
28. Moe PC, Heuck AP. Phospholipid hydrolysis caused by Clostridium perfringens alpha-toxin facilitates the targeting of perfringolysin O to membrane bilayers. Biochemistry 2010;49:9498–507.
29. Diaz R, Mayorga L, Stahl P. In vitro fusion of endosomes following receptor-mediated endocytosis. J Biol Chem 1988;263:6093–100.
30. Yunes R, Michaut M, Tomes C, Mayorga LS. Rab3A triggers the acrosome reaction in permeabilized human spermatozoa. Biol Reprod 2000;62:1084–9.
31. Bello OD, Zanetti MN, Mayorga LS, Michaut MA. RIM, Munc13, and Rab3A interplay in acrosomal exocytosis. Exp Cell Res 2012;318:478–88.
32. Steck TL, Lange Y. Cell cholesterol homeostasis: mediation by active cholesterol. Trends Cell Biol 2010;20:680–7.
33. Flanagan JJ, Tweten RK, Johnson AE, Heuck AP. Cholesterol exposure at the membrane surface is necessary and sufficient to trigger perfringolysin O binding. Biochemistry 2009;48:3977–87.
34. Sokolov A, Radhakrishnan A. Accessibility of cholesterol in endoplasmic reticulum membranes and activation of SREBP-2 switch abruptly at a common cholesterol threshold. J Biol Chem 2010;285:29480–90.
35. Nelson LD, Johnson AE, London E. How interaction of perfringolysin O with membranes is controlled by sterol structure, lipid structure, and physiological low pH: insights into the origin of perfringolysin O-lipid raft interaction. J Biol Chem 2008;283:4632–42.
36. Selvaraj V, Asano A, Buttke DE, Sengupta P, Weiss RS, Travis AJ. Mechanisms underlying the micron-scale segregation of sterols and GM1 in live mammalian sperm. J Cell Physiol 2009;218:522–36.
37. Branham MT, Bustos MA, De Blas GA, Rehmann H, Zarelli VE, Trevino CL, et al. Epac activates the small G proteins Rap1 and Rab3A to achieve exocytosis. J Biol Chem 2009;284:24825–39.
38. Castillo BJ, Roggero CM, Mancifesta FE, Mayorga LS. Calcineurin-mediated dephosphorylation of synaptotagmin VI is necessary for acrosomal exocytosis. J Biol Chem 2010;285:26269–78.
39. Sanyal S, Claessen JH, Ploegh HL. A viral deubiquitylating enzyme restores dislocation of substrates from the ER in semi-intact cells. J Biol Chem 2012;287:23594–603.
40. Kleba B, Stephens RS. Chlamydial effector proteins localized to the host cell cytoplasmic compartment. Infect Immun 2008;76:4842–50.
41. Weng N, Baumler MD, Thomas DD, Falkowski MA, Swayne LA, Braun JE, et al. Functional role of J domain of cysteine string protein in Ca^{2+}-dependent secretion from acinar cells. Am J Physiol Gastrointest Liver Physiol 2009;296:G1030–9.
42. Falkowski MA, Thomas DD, Groblewski GE. Complexin 2 modulates vesicle-associated membrane protein (VAMP) 2-regulated zymogen granule exocytosis in pancreatic acini. J Biol Chem 2010;285:35558–66.
43. Batiz LF, De Blas GA, Michaut MA, Ramirez AR, Rodriguez F, Ratto MH, et al. Sperm from hyh mice carrying a point mutation in aSNAP have a defect in acrosome reaction. PLoS ONE 2009;4:e4963.

SUPPLEMENTAL MATERIALS

MATERIALS AND METHODS

Reagents

Ni-NTA-agarose was from Qiagen (Tecnolab SA); DL- dithiothreitol (DTT), isopropyl β-D-1-thiogalactopyranoside (IPTG), and *Pisum sativum* agglutinin conjugated with fluorescein isothiocyanate (PSL-FITC) were from ICN (Eurolab SA); digitonin was from Sigma (Sigma-Aldrich Argentina SA); propidium iodide and eosin Y were from Molecular Probes (Invitrogen Argentina Ltd.). Mouse anti-His_6 antibody was from Calbiochem (MERCK Química Argentina SAIC); horseradish peroxidase (HRP)-coupled anti-mouse antibody and Cy3-labeled goat anti-mouse antibody were from Jackson Immunochemicals (Sero-immuno Diagnostics, Inc.); rabbit polyclonal anti-Rab3A antibody (purified IgG) was from Santa Cruz Biotechnology, Inc.; anti-complexin I/II (rabbit polyclonal, purified IgG) was from Synaptic Systems; rabbit polyclonal antibody against Epac was from Genemed Synthesis, Inc.

Recombinant Proteins

Recombinant protein concentrations were determined by the Bio-Rad protein assay in 96-well microplates. BSA was used as a standard, and the results were quantified on a 3550 Microplate Reader (Bio-Rad). PFO (about 1 μM) was divided in 15-μL aliquots and stored at −80°C in the elution buffer. Under these storage conditions, PFO was stable and fully active for at least 6 months. The plasmid encoding the Rab3-GTP binding cassette of RIM1α (residues 1-399, RIM-RBD) fused to GST was kindly provided by Dr. Regazzi (University of Lausanne, Switzerland). The plasmid encoding Rab3A fused to GST was generously provided by Dr. P. Stahl (Washington University, St. Louis, MO). All plasmids fused to GST in pGEX-2T or pGEX-KG vectors were transformed in BL21 (DE3) cells (Stratagene), and expression was induced overnight at 22°C with 0.5 mM IPTG. Recombinant proteins were purified by affinity chromatography on glutathione-sepharose beads as described elsewhere (1). Rab3A was prenylated and loaded with guanosine 5′-[γ-thio] triphosphate as described by Yunes et al. (2).

PFO Binding to Sperm Plasma Membrane Assessed by Indirect Immunofluorescence

Capacitated and noncapacitated spermatozoa were washed twice, resuspended in ice-cold PBS containing 25 nM PFO, and incubated for 15 minutes at 4°C. After washing twice with PBS to remove the free toxin, the cells were fixed in 2% paraformaldehyde in PBS for 10 minutes at 4°C and spotted on poly-L-lysine-covered slides. After air drying, sperm were incubated in 50 mM glycine PBS for 30 minutes at 22°C and then for 30 minutes in 5% BSA-PBS. Spermatozoa were labeled with a mouse anti-His_6 antibody (1:50 in 1% BSA-PBS) overnight at 4°C, followed by a Cy3-labeled anti-mouse IgG as a secondary antibody (1:600 in 1% BSA-PBS) for 1 hour at 22°C. Slides were washed with PBS between incubations. Finally, slides were mounted in 1% propyl-gallate/50% glycerol in PBS and analyzed using a Nikon EZ-C1 confocal microscope with the EZ-C1 Gold Version 3.90 built 869 software and a Plan Apo 60×/1.40 oil Nikon objective. Images were processed using Image J (National Institutes of Health, http://rsb.info.nih.gov/ij/).

PFO Binding to Sperm Plasma Membrane Assessed by Western Blot

Capacitated and noncapacitated spermatozoa were washed twice, resuspended in ice-cold PBS containing 25 nM PFO, and incubated for 15 minutes at 4°C. After washing twice with PBS to remove the free toxin, sperm pellets (10×10^6 cells) were resuspended in sample buffer (2% SDS, 10% glycerol, 62.5 mM Tris-HCl) without disulfide-reducing agents. Proteins were extracted by heating the pellet in sample buffer twice to 95°C for 6 minutes each. Extracts were centrifuged ($12{,}000 \times g$) for 10 minutes, and the supernatants were adjusted to 5% β- mercaptoethanol, boiled for 3 minutes, and used immediately or stored at −20°C. Proteins were separated on 10% tris-tricine gel and transferred to nitrocellulose membrane (Hybond-ECL, GE Healthcare). Nonspecific reactivity was blocked by incubation for 1 hour at 22°C with 1% skim milk in washing buffer (0.1% Tween 20 in PBS). Blots were incubated with a mouse anti-6 His antibody (1:5,000) in washing buffer for 1 hour at 22°C. HRP-conjugated goat anti-mouse IgG was used as a secondary antibody (1:2,000, in washing buffer, 1 hour at room temperature). Excess first and second antibodies were removed by washing the nitrocellulose membranes 5 × 5 minutes in washing buffer. Detection was accomplished with Western Lightning Chemiluminiscence Reagent Plus (Perkin Elmer). The images of the bands were obtained using a Luminescent Image Analyzer LAS-4000 (Fujifilm).

Single-Cell Experiments: PFO Permeabilization in Real Time

Sperm were adjusted to a concentration of 10×10^6 and immobilized on poly-L-lysine-coated round coverslips (0.001% poly-L-lysine drops were air dried followed by one rinse with water), which were mounted on a chamber and placed on the stage of an inverted Eclipse TE300 Nikon microscope. LED output was synchronized to the Exposure Out signal of a Luca R EMCCD camera (Andor Technology). Images were collected (6 frames/minute) using NIS Element software (Nikon) and a Plan Fluor 40×/0.6 Nikon objective. Images were processed using Image J. Any incompletely adhered sperm that moved during the course of the experiment were discarded. Fluorescence measurements in individual sperm were made by manually drawing a region of interest around the head of each cell. When required, raw intensity values were normalized using $(F - FL)/(FH - FL) \times 100$, where F is fluorescence intensity at time *t*, FL is the lower fluorescence, and FH is the higher fluorescence taken during the experiments. The normalized fluorescence versus time series were fitted to cumulative Gaussian curves using the nonlinear routine of GraphPad Prism version 5.00 for Windows (GraphPad Software).

Acrosomal Exocytosis in PFO Permeabilized Sperm

Human semen samples were process under capacitated conditions and incubated (when appropriate) with 25 nM PFO as described above. Sperm were washed with cold PBS, resuspended (7×10^6/mL) in ice-cold HB-EGTA buffer containing 2 mM DTT, and divided in 50-μL aliquots. We added inhibitors and stimulants sequentially without washing as indicated in the figure legends and incubated them for 10 minutes at 37°C after each addition. Care was taken to maintain the same incubation times for all tubes in the same experiment. Intact and permeabilized sperm were spotted on Teflon-printed slides, air dried, and fixed/permeabilized in ice-cold methanol for 1 minute. Acrosomal status was evaluated by staining with PSL-FITC. At least 200 cells were scored using an upright Nikon microscope equipped with epifluorescence optics. Basal (no stimulation) and positive (0.5 mM $CaCl_2$ corresponding to 10 μM free calcium for permeabilized cells and 10 μM A23187 for intact cells) controls were included in all experiments. For each experiment, acrosomal exocytosis indexes were normalized by subtracting the number of reacted spermatozoa in the negative control (range, 18%–30%) from all values and expressing the resulting values as a percentage of the acrosome reaction observed in the positive control (range, 30%–50%). The average difference between positive and negative controls was 14% (experiments for which the difference was less than 10% were discarded).

REFERENCES

1. Branham MT, Bustos MA, De Blas GA, Rehmann H, Zarelli VE, Trevino CL, et al. Epac activates the small G proteins Rap1 and Rab3A to achieve exocytosis. J Biol Chem 2009;284:24825–39.
2. Yunes R, Michaut M, Tomes C, Mayorga LS. Rab3A triggers the acrosome reaction in permeabilized human spermatozoa. Biol Reprod 2000;62:1084–9.